  Bull. Chem. Soc. Jpn., 63, 3385—3397 (1990)

Femtosecond-Picosecond Laser Photolysis Studies on Photoreduction Process of Excited Benzophenone with *N,N*-Dimethylaniline in Acetonitrile Solution

Hiroshi MIYASAKA, Kazuhiro MORITA, Kenji KAMADA, and Noboru MATAGA*
Department of Chemistry, Faculty of Engineering Science, Osaka University, Toyonaka, Osaka 560
(Received August 3, 1990)

Photoreduction processes of excited benzophenone (BP) by *N,N*-dimethylaniline (DMA) in acetonitrile solution were studied by means of picosecond-femtosecond laser photolysis and time resolved transient absorption spectroscopy as well as transient photoconductivity measurement. Proton transfer process in the triplet ion pair formed by electron transfer (ET) at encounter between ^{3}BP* and DMA, competing with the ionic dissociation process was observed. It was clearly demonstrated that, in addition to the triplet ion pair, the ion pair produced by the excitation of the CT complex between BP and DMA formed in the ground state and that produced by ET reaction between ^{1}BP* and DMA played important roles in the reaction processes of excited benzophenone. The behaviors of the three kinds of ion pairs were investigated in detail, leading to the elucidation of reaction mechanism of each ion pair. The reactivity characteristic of each kind of the ion pair and its relation to the structure of the ion pair were discussed.

The photoinduced electron transfer (ET) and related processes are of fundamental importance in photophysical and photochemical reaction processes in condensed phase.[1-4] The photoreduction of excited benzophenone in solution is one of the most important photochemical reaction related to this fundamental process and has been studied extensively for a long time.[5-16] Especially, much attention has been paid to the hydrogen abstraction process of excited triplet benzophenone (^{3}BP*) from aliphatic as well as aromatic amines. The yield of the ketyl radical in the reaction of ^{3}BP* with the amine is usually very high and the reaction rate is rather close to that of the diffusion-controlled reaction, while the rate for the hydrogen abstraction from 2-propanol is about 10^3 times smaller than those from amines. On the basis of such results, Cohen et al. proposed[7] the reaction mechanism for the hydrogen abstraction of ^{3}BP* from amines, which assumed the CT complex or ion pair formation followed by proton transfer;

$$^3\mathrm{BP}^* + \mathrm{AH} \xrightarrow[\text{transfer}]{\text{electron}} {}^3(\mathrm{BP}^- \cdots \mathrm{AH}^+) \xrightarrow[\text{transfer}]{\text{proton}} (\mathrm{BPH} + \mathrm{A}),$$

where AH is an amine and BPH is a ketyl radical.

In an early research by means of a nanosecond laser photolysis,[8,9] it was suggested that the CT or the ion pair (IP) state prior to the solvation was the species undergoing the proton transfer leading to the BPH formation, i.e., the proton transfer in the IP state competed with the solvatlon leading to the ionic dissociation.

The direct measurement on the picosecond dynamics of the excited benzophenone and the amine system was reported by Peters and co-workers.[10-13] On the basis of the observed time-dependent spectral shift of the benzophenone anion radical, they concluded that the structural change of the solvent separated IP formed by the ET between ^{3}BP* and amine, to the contact IP was the key process for the proton transfer to take place.

On the other hand, we have recently reported the results of the picosecond laser photolysis studies on the reaction of the excited benzophenone with diphenylamine (DPA) in several solvents of different polarity.[16] In this investigation, it was demonstrated that the hydrogen abstraction and charge transfer (CT) or ion pair (IP) state formation by electron transfer were competing at encounter between triplet benzophenone (^{3}BP*) and DPA both in nonpolar and polar solvent, and the CT or IP state relaxed with respect to the donor acceptor configurations and solvation did not contribute to the ketyl radical formation. In addition to this, it was also revealed that the ET reaction of benzophenone in its excited singlet state (^{1}BP*) and the ion pair formation by the excitation of the CT complex produced in the ground state were very important in considering the mechanism of the photoreduction of the excited benzophenone.

It is plausible that the properties of those IP's such as the rate of proton transfer and that of the charge recombination depend on their structures (the distance between the ions in the pair and their mutual orientations including the surrounding solvents), energy gap between the IP and ground state and spin multiplicity, etc. In fact, recent investigation on the CR rates of IP revealed that the CR rate of IP formed by excitation of various CT complexes showed an essentially different energy gap dependence from the bell-shaped one obtained in the case of IP formed by charge separation (CS) at encounter in the fluorescence quenching reaction.[17] Hence, it is absolutely necessary to discriminate the different kind ion pairs and their subsequent reactions for the elucidation of the photoreduction process of the excited benzophenone, especially in the concentrated solution of the amine.

In this study, we have examined the photoreduction process of excited benzophenone by *N,N*-dimethylaniline (DMA) in acetonitrile solution by means of picosecond and femtosecond laser photolysis. As will be presented later, IP produced by the CT band excitation of the ground state complex, IP formed by CS at encounter between ^{1}BP* and DMA, and that produced by CS at encounter between ^{3}BP* and DMA exhibit quite different behaviors dependent on the mode of the production. On the basis of those experimental results, the different reactivity of IP dependent on the mode of its formation and on its spin multiplicity will be discussed. In addition, the conventional mechanisms of the hydrogen abstraction reaction of ^{3}BP* will be reconsidered including the contributions from ^{1}BP* and the excited state of BP-amine CT complex.

Experimental

A picosecond laser photolysis system with a repetitive mode-locked Nd^{3+} : YAG laser was used for transient absorption spectral measurements in the 10 ps to a few nanosecond region.[18,19] The third harmonic pulse (355 nm) with 22 ps fwhm or Raman scattering light (397 nm) obtained by focusing the 355 nm pulse into cyclohexane liquid was used for exciting the sample solutions. The method for the picosecond laser-induced transient photoconductivity measurements was similar to those reported before.[20] For the measurement in short time region, a femtosecond laser system was used.[4,21] In this femtosecond photolysis, second harmonics (355 nm) with 500 fs fwhm of pyridine 1 dye laser (710 nm) was used for the excitation.

Benzophenone (Wako, Special Guarantee) was purified by repeated recrystallization from ethanol and sublimation in a vacuum. *N,N*-dimethylaniline (DMA) (Wako, Special Guarantee) was refluxed with acetic anhydride, washed with water, dried over potassium hydroxide, distilled under reduced pressure, and stored under vacuum. Acetonitrile (Merck Uvasol) was used without further purification for the time resolved transient absorption spectral measurements. In the measurement of laser-induced transient photoconductivity, this solvent was dried by contacting with molecular sieves and distilled in a vacuum. All sample solutions were deaerated by repeated freeze-pump-thaw cycles. The BP solution and DMA were deaerated separately and DMA was added to the BP solution by distillation in a vacuum line. All measurements were performed at 22±2 °C.

The extinction coefficients used for the estimation of the reaction yields are as follows; 6500 M^{-1} cm^{-1} at ca. 525 nm for ^{3}BP*, 4600 M^{-1} cm^{-1} at 545 m for BPH, and 10000 M^{-1} cm^{-1} for BP^- around 700 nm. Detailed discussion on the determination of the extinction coefficient of each species was presented in the previous paper.[16]

Results and Discussion

As mentioned in the introductory section, there exist at least three pathways leading to the ion pair formation: (1) the excitation of the weak CT complex formed in the ground state, $^1(BP^-\cdots DMA^+)_{com}$, (2) the electron transfer (ET) reaction between the excited singlet benzophenone (^{1}BP*) and DMA, $^1(BP^-\cdots DMA^+)_{enc}$, and (3) the ET reaction between ^{3}BP* and DMA, $^3(BP^-\cdots DMA^+)_{enc}$. It is of crucial importance to get precise information on the role played by each ion pair for the elucidation of the reaction mechanisms of the photoreduction processes of benzophenone.

In the following, first, we examine the reaction of ^{3}BP* with DMA leading to the ketyl radical formation and make clear the role of the triplet ion pair in this reaction. Second, we demonstrate the CT complex formation between BP and DMA in the ground state and the dynamic behaviors of this complex in its excited state. Third, we show results obtained by femtosecond laser photolysis, where the ET reaction of ^{1}BP* and DMA is discussed. Finally, we discuss the differences among the reactivities of ^{1}BP*, ^{3}BP*, and three kinds of ion pairs by integrating the experimental results obtained here.

1. Photoreduction Processes of ^{3}BP* by DMA in Acetonitrile Solution. Figure 1 shows the time

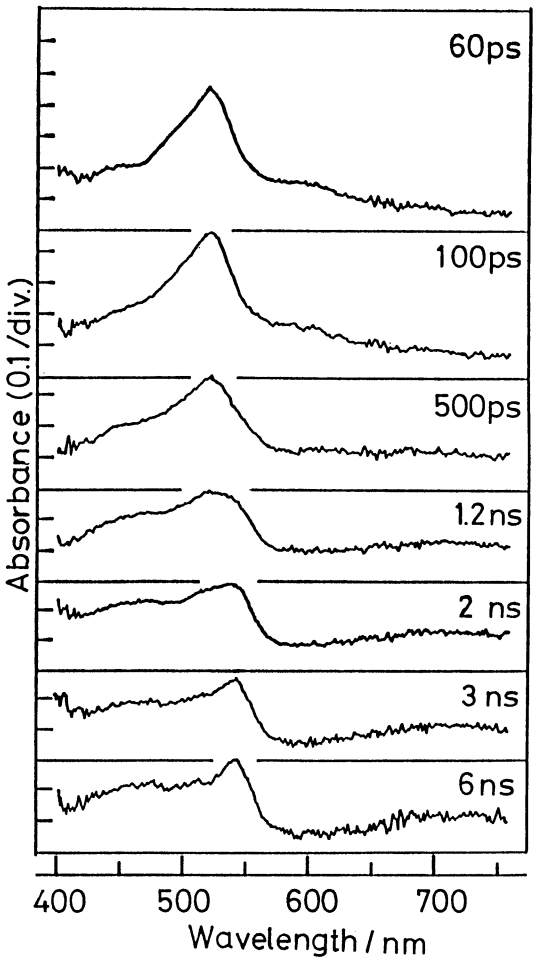

Fig. 1. Time-resolved transient absorption spectra of BP(0.01 M)-DMA(0.05 M) system in acetonitrile solution excited with a picosecond 355 nm laser pulse.

resolved transient absorption spectra of BP(0.01 M)-DMA(0.05 M) (1 M=1 mol dm^{-3}) system in acetonitrile solution excited with a picosecond 355 nm laser pulse. A transient absorption spectrum with an absorption maximum at 525 nm, which is assigned to ^{3}BP*,[22] decreases with increase of the delay time after the excitation and new bands at 475 nm, 545 nm, and ca. 700 nm appear. These new absorption bands can be assigned to each species as follows; the 545 nm band to BPH,[5,23] the 475 nm band to DMA$^+$,[24] and that at 700 nm to BP$^-$,[25] respectively. The transient absorption spectra in Fig. 1 indicate that ^{3}BP* gradually evolves with increase of the delay time into BPH formed by the hydrogen abstraction reaction and ^{3}(BP$^-$···DMA$^+$) produced through the electron transfer reaction.

In Fig 2, we exhibit the time profiles of ^{3}BP*, BPH and ^{3}(BP$^-$···DMA$^+$), which were obtained by analysing the observed spectra into these three components on the basis of their individual reference spectra. In this figure, the ordinate represents the concentration of the individual species calculated by using each extinction coefficient given in the Experimental. As shown in this figure, the decay time of ^{3}BP* coincides with the rise time of BPH radical and the yield of BPH from ^{3}BP* was obtained to be 0.73. The concentrations of ion pairs also show gradual increase along with the decay of ^{3}BP*. Since the observed rise of the photoconductivity was nearly equal to the response of the apparatus (a few ns), the absorption signal ascribed to ionic species in a few ns after the excitation is mainly due to the dissociated ions. The yield of the ionic dissociation was 0.17.

We have examined also the solution of BP in acetonitrile containing DMA of higher concentration (0.3 M) by picosecond laser photolysis exciting with 355 nm laser pulse (Fig. 3). As can be observed in Fig. 3, the concentration of ^{3}BP* with its absorption maximum at 525 nm decreases and that of BPH radical with its absorption maximum at 545 nm increases with increase of the delay time after the excitation. It should be noted here that the transient absorption spectrum at early stage after the excitation shows a rather large amount of the absorption signal due to

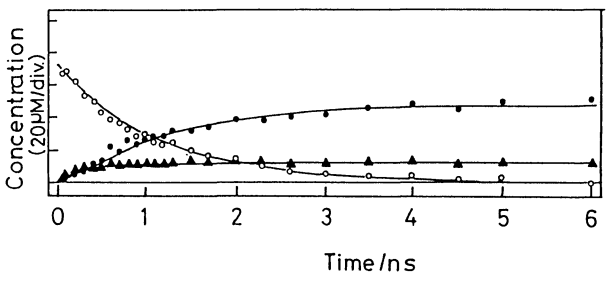

Fig. 2. Time profiles of ^{3}BP* (○), BPH (●), and BP$^-$ and DMA$^+$ (▲) of BP(0.01 M)-DMA(0.05 M) system in acetonitrile solution excited with a picosecond 355 nm laser pulse (see text).

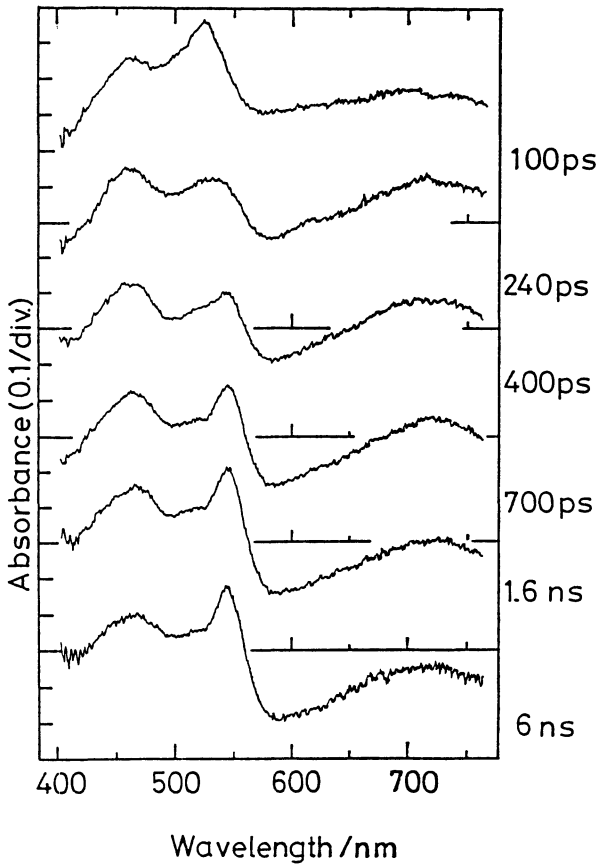

Fig. 3. Time-resolved transient absorption spectra of BP(0.01 M)-DMA(0.3 M) system in acetonitrile solution excited with a picosecond 355 nm laser pulse.

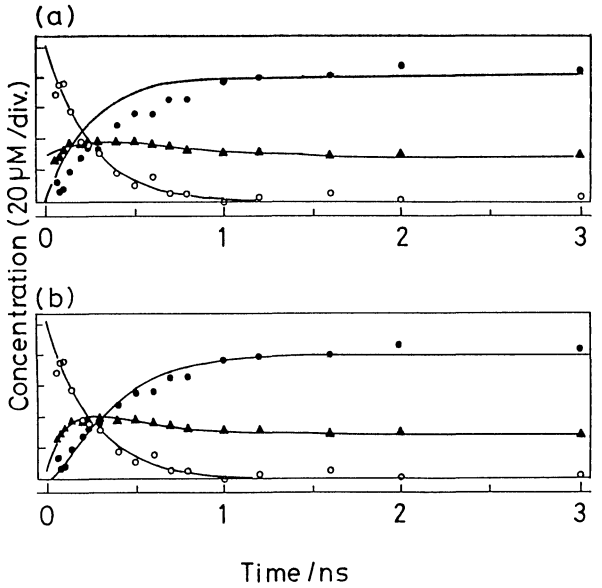

Fig. 4. Time profiles of ^{3}BP* (○), BPH (●), and BP$^-$ and DMA$^+$ (▲) of BP (0.01 M)-DMA(0.3 M) system in acetonitrile solution excited with a picosecond 355 nm laser pulse (see text). Solid lines are calculated curves based on Scheme 1(a), and on Scheme 2(b) (see text).

$(BP^{-}\cdots DMA^{+})$ compared to that observed in the solution containing 0.05 M DMA. This rapid production of ion pairs is partly due to the formation of $^{1}(BP^{-}\cdots DMA^{+})_{enc}$, via the electron transfer reaction between $^{1}BP^{*}$ and DMA, and the formation of $^{1}(BP^{-}\cdots DMA^{+})_{com}$, by the excitation of the CT complex formed in the ground state. More details on these species will be described later.

Figure 4 shows the time profiles of three kinds of transient species, $^{3}BP^{*}$, BPH, and ion pairs, obtained by the analysis of the spectra in Fig. 3 with the same method as used in the analysis of the spectra in Fig. 1. Solid lines in Fig. 4(a) exhibit the calculated curves on the basis of the following reaction scheme,

$$^{3}BP^{*} + DMA \rightarrow {}^{3}(BP^{-}\cdots DMA^{+})_{enc} \rightarrow BP^{-}_{s} + DMA^{+}_{s}$$
$$\qquad\qquad \rightarrow (BPH^{\cdot}\cdots DMA^{\cdot}) \rightarrow BPH^{\cdot} + DMA^{\cdot}$$

Scheme 1.

where $DMA^{\cdot}$ indicates the neutral radical produced after the abstraction of a hydrogen atom from DMA. We can see clearly from the results in this figure that rise of BPH radical is slower than the decay of $^{3}BP^{*}$, and the time profiles of $^{3}BP^{*}$ and BPH radical cannot be reproduced consistently by the calculated curves based on the Scheme 1. Accordingly, the mechanism of Scheme 1 is not adequate to the reaction of $^{3}BP^{*}$ with DMA in acetonitrile solution, although this direct abstraction mechanism competing with the ion pair formation was suitable for the hydrogen abstraction process of $^{3}BP^{*}$ from diphenylamine.[16]

On the other hand, the time profiles calculated on the basis of the Scheme 2 are indicated in Fig. 4(b).

$$^{3}BP^{*} + DMA \rightarrow {}^{3}(BP^{-}\cdots DMA^{+})_{enc} \rightarrow BP^{-}_{s} + DMA^{+}_{s}$$
$$\qquad\qquad \rightarrow (BPH^{\cdot}\cdots DMA^{\cdot}) \rightarrow BPH^{\cdot} + DMA^{\cdot}$$

Scheme 2.

Scheme 2 represents the successive mechanism for the hydrogen atom transfer; the ion pair produced by the electron transfer proceeds to proton transfer reaction competing with the ionic dissociation process. The parameters for the transient species such as the lifetime of the triplet ion pair and reaction yields of the proton transfer and the ionic dissociation were determined respectively in such a manner that the time profiles of $^{3}BP^{*}$, BPH radical, and the ion pair were consistent with each other. In addition, parameters such as the lifetimes of the singlet ion pairs, their initial yields, and their proton transfer reaction yields were also included in this curve fitting-procedure. More details on the singlet ion pairs will be described in the later part of this paper.

As shown in Fig. 4(b), the time profile of each species is well reproduced by the calculated curve based on the Scheme 2. The lifetime of $^{3}(BP^{-}\cdots DMA^{+})_{enc}$ was 130 ps, and the reaction yield of the proton transfer and that of the ionic dissociation were 0.75 and 0.22, respectively. These reaction yields were in accordance with those obtained for the solution containing 0.05 M DMA (Fig. 1 and 2). In this way, the consecutive reaction mechanism (Scheme 2) for the reaction of $^{3}BP^{*}$ with DMA in acetonitrile was found to fit the observed time profiles over a wide range of DMA concentration.

The lifetime of the ion pair, reaction yields and rate constants for the proton transfer and the ionic dissociation in acetonitrile solution with various concentrations of DMA, which were obtained by this curve-fitting procedure, are listed in Table 1. Results in this table show clearly that similar values were obtained for the ion pair lifetime and the reaction yields over a wide range of the DMA concentration. This fact indicates that the reaction mechanism for the hydrogen abstraction reaction of $^{3}BP^{*}$ from DMA in acetonitrile solution can be described by Scheme 2. In addition, the rate constant for the ionic dissociation, 1.4×10^{9} s^{-1}, was similar to those obtained for a number of organic radical ion pairs produced by the electron transfer at encounter collision.[26] This result also shows that the values of the lifetime and reaction yields of $^{3}(BP^{-}\cdots DMA^{+})_{enc}$ obtained by this analysis and the extinction coefficients used here are appropriate.

Peters et al. also reported the results of the picosecond laser photolysis studies[12] on the photoreduction process of the excited benzophenone by DMA in acetonitrile solution. Although the reaction scheme concluded from the results in the present work is

Table 1. Properties of $^{3}(BP^{-}\cdots DMA^{+})_{enc}$, in Acetonitrile Solutions with Various Concentrations of DMA. τ: Lifetime, ϕ_{PT} and k_{PT}: Reaction Yield and Rate Constant of the Proton Transfer, ϕ_{ID} and k_{ID}: Reaction Yield and Rate Constant for the Ionic Dissociation

[DMA]	τ/ps	ϕ_{PT}	ϕ_{ID}	k_{PT}/s^{-1}	k_{ID}/s^{-1}
0.05 M	150	0.73	0.17	4.9×10^{9}	1.1×10^{9}
0.1 M	150	0.72	0.18	4.9×10^{9}	1.2×10^{9}
0.3 M	130	0.75	0.22	5.8×10^{9}	1.7×10^{9}
0.6 M	140	0.76	0.21	5.4×10^{9}	1.5×10^{9}
1.0 M	120	0.73	0.16	6.1×10^{9}	1.3×10^{9}
Average	(140±13)	0.74±0.016	0.19±0.026	$(5.4\pm0.51)\times10^{9}$	$(1.4\pm0.23)\times10^{9}$

similar to theirs, the ion pair lifetime and reaction yields obtained by them are quite different from ours. This is because they ignored the contribution of the singlet ion pairs to the reaction even in the very concentrated solution of DMA (1.0—5.0 M). This problem of the singlet ion pairs will be discussed in detail in the later part of this paper.

In any way, the hydrogen abstraction of ^{3}BP* from DMA in acetonitrile solution can be described by the reaction mechanism of Scheme 2 which is different from the mechanism of the reaction where the diphenylamine is used as hydrogen donor.[16] This difference may be ascribed to the difference in the structure between the secondary and tertiary amine. In addition, the structure of the intermediate ion pair state, which depends on the oxidation potential of the amine and the solvent, may affect the reaction mechanism. For example, the hydrogen abstraction of ^{3}BP* from DMA in 2-propanol was found to be described by the reaction mechanism of Scheme 1.[27]

2. Excited State Dynamics of the Weak CT Complex Formed in the Ground State. Figure 5 shows the ground state absorption spectra of BP (0.05 M) and DMA in acetonitrile. The absorbance in the wavelength region longer than 350 nm, especially the absorption tail in the region longer than 380 nm, increases with increase of concentration of DMA. This change of absorption spectrum can be attributed to the weak CT complex formation between BP and DMA in the ground state, since the excitation at the absorption tail leads to the rapid formation of the ion pair, ^{1}(BP$^-$···DMA$^+$)$_{com}$ (see Fig. 6). The equiriblium constant of this complex formation, K_g, was estimated to be 0.1—0.5 by Benesi-Hildebrand plot.

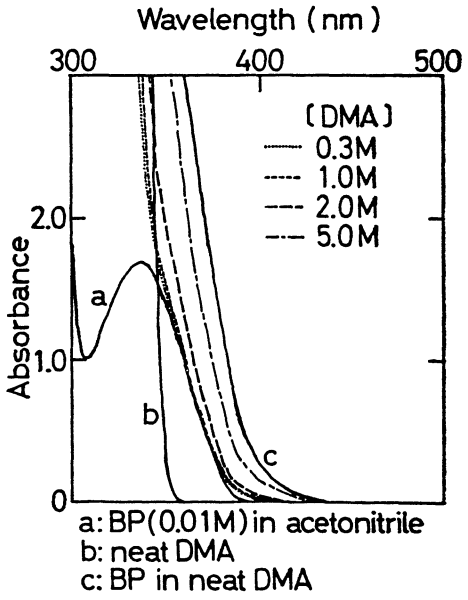

Fig. 5. Effect of DMA concentration on the ground state absorption of benzophenone in acetonitrile.

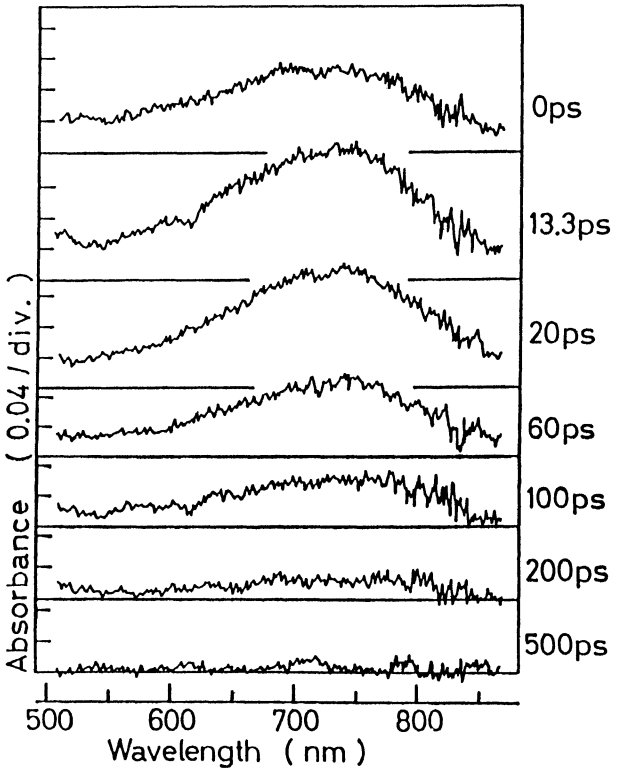

Fig. 6. Time-resolved transient absorption spectra of BP(0.5 M)-DMA(1.0 M) system in acetonitrile excited with a picosecond 397 nm laser pulse.

In Figure 6, we show transient absorption spectra of BP (0.5 M)-DMA (1.0 M) system in acetonitrile solution excited with a picosecond 397 nm laser pulse. The irradiation at this wavelength selectively excites the ground state complex as can be seen from Fig. 5. This figure indicates that a broad absorption spectrum with an absorption maximum around 740 nm arises immediately after excitation, followed by rapid decrease. This absorption spectrum was safely assigned to BP$^-$ on the basis of the absorption maximum and the spectral shape.[25] Hence, the absorption spectra in Fig. 6 indicate that the excitation of the CT complex gives the transient ion pair state which undergoes rapid charge recombination (CR) decay. The decay process was confirmed to obey the first order kinetics and the time constant was determined to be (85±3) ps. After the decay of the ion pair, no absorption due to BPH was detected. The yield of the ionic dissociation was estimated to be <3%. Accordingly, the CR process is the dominant pathway in the decay of the ion pair ^{1}(BP$^-$···DMA$^+$)$_{com}$. It has been reported that the peak position of BP$^-$ absorption moves depending on the structure of the ion pair and the degree of solvation.[28,29] In the present study, however, no spectral shift of BP$^-$ absorption was observed in the course of the CR decay. Therefore, it may be concluded that the structure of the present ion pair is unchanged in this recombination process.

Summarizing above results, we may conclude that the ion pair produced by the excitation of the weak CT complex formed in the ground state, $^1(BP^-\cdots DMA^+)_{com}$, results in the rapid CR decay without proton transfer or effective ionic dissociation.

The rapid recombination of the ion pair produced by the CT band excitation without proton transfer reaction can explain the following experimental results concerned with the yield of BPH radical. First, it has been widely known that the increase of the concentration of the amine reduces the yield of benzopinacol which is the final product formed by reaction between BPH radicals.[7] This well-known fact is interpreted by the present picosecond experimental results that the increase of the amine concentration facilitate the formation of the CT complex whose reaction yield of BPH formation is practically zero. Second, Pac et al. concluded on the basis of the analysis of the photoproduct that the excitation at the CT band of the complex between the BP and some amines results in no permanent products formation.[30] This result can be also explained by taking into account the short-lived transient ion pair produced by the CT band excitation. The structure of this ion pair state and dependences of the reactivity and the lifetime of the ion pair on its structure will be discussed later.

3. Photoreduction Processes of $^1BP^*$ by DMA in Acetonitrile Solution. In addition to the charge separation through the excited CT complex, the ion pair formation at encounter in the fluorescence quenching reaction of $^1BP^*$ was also effective in the concentrated solution of amine.[16]

Prior to the discussion on the electron transfer process of $^1BP^*$, we show results of our measurements on the $S_n \leftarrow S_1$ absorption spectrum and the intersystem crossing (ISC) process of benzophenone in Fig. 7, where the time resolved transient absorption spectra of BP in acetonitrile (a), and in isooctane (b) excited with a 500 fs 355 nm laser pulse are exhibited. The transient absorption spectrum with an absorption maximum around 575 nm was observed immediately after the excitation in each solution. With increase of the delay time after the excitation, the absorption spectrum with a peak at ca. 525 nm increases. The latter can be safely assigned to the $T_n \leftarrow T_1$ absorption spectrum of benzophenone on the basis of the coincidence of the absorption maximum and spectral shape to the $T_n \leftarrow T_1$ absorption spectrum which we have observed in each solvent.[16]

On the other hand, the former spectrum observed immediately after the excitation may be ascribed to the $S_n \leftarrow S_1$ transition of benzophenone on the following reasons. First, this absorption spectrum appeared with the time constant almost identical with the response function of the apparatus. Second, this absorption spectrum was gradually converted into the $T_n \leftarrow T_1$ absorption spectrum and the time constant for this change was independent of the wave-

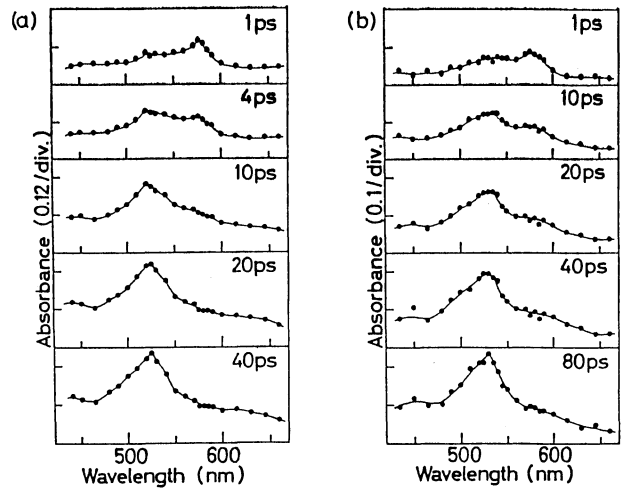

Fig. 7. Time-resolved transient absorption spectra of BP(0.05 M) in acetonitrile (a), and in isooctane (b), measured by exciting with a 500 fs 355 nm laser pulse.

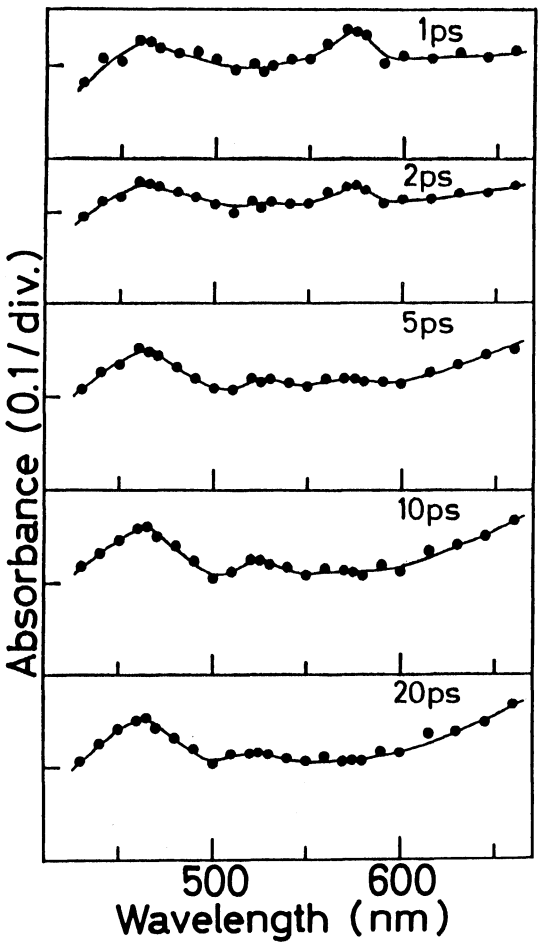

Fig. 8. Time-resolved transient absorption spectra of BP(0.05 M)-DMA(1.0 M) system in acetonitrile, measured by exciting with a 500 fs 355 nm laser pulse.

length. The rise time of the $T_n \leftarrow T_1$ absorption (intersystem crossing (ISC) time) was obtained to be (9±2) ps in acetonitrile solution and (16±2) ps in isooctane solution, respectively. These values are very close to the ISC rates obtained previously[31] by picosecond laser photolysis. The extinction coefficient of the $S_n \leftarrow S_1$ absorption at 575 nm was estimated to be (3600±450) $M^{-1}cm^{-1}$ by using the following values; 1.0 for the quantum yield of ISC and 6500 M^{-1} s^{-1} for the extinction coefficient of the $T_n \leftarrow T_1$ absorption at 525 nm, respectively.

Figure 8 shows the time resolved transient absorption spectra of BP-DMA (1.0 M) in acetonitrile solution excited with a femtosecond 355 nm laser pulse. A transient absorption spectrum at 1 ps after the excitation clearly indicates absorption maxima at 470 nm and 575 nm. In addition to these two peaks, a broad absorption whose intensity increases toward longer wavelength region than 600 nm is also observed. The band with a maximum at 575 nm can be ascribed to the $S_n \leftarrow S_1$ transition of BP. On the other hand, the absorption band at 470 nm and the broad absorption with increasing intensity toward longer wavelength than 600 nm are respectively assigned to DMA^+ and BP^- in the ion pair. This rapid formation of the ion pair is due to the excitation at the CT band overlapping the ground state absorption band of free BP, as stated in the previous section. With increase of the delay time, the absorption at 575 nm decreases and the absorption due to the ion pair gradually increases together with the increase of a new band at 525 nm which is due to $^3BP^*$.

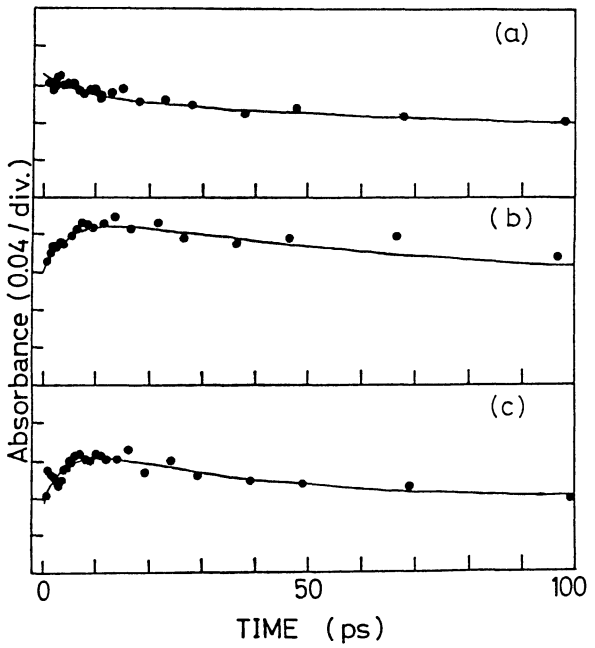

Fig. 9. Time profiles of transient absorbance of BP(0.05 M)-DMA(1.0 M) system in acetonitrile excited with a 500 fs 355 nm laser pulse and observed at 575 nm (a), 670 nm (b), and 525 nm (c).

Time profiles of transient absorbance at 575 nm, 670 nm, and 525 nm are exhibited in Fig. 9. The absorbance at 575 nm corresponding to the absorption maximum of $^1BP^*$ appears within the time resolution of the apparatus, followed by a rapid decay with time constant of (5.0±1.0) ps and a much slower decay whose time constant is longer than a few tens of picoseconds. The former (rapid decay) can be attributed to the quenching process of $^1BP^*$ by amine and the latter (slow decay) may be due to the decay of $^3BP^*$ and ion pairs with their absorption bands overlapping at this wavelength. The lifetime of $^1BP^*$ was reduced to 5.0 ps in 1.0 M DMA solution compared to the much longer lifetime of 9.0 ps of the amine free solution. On the other hand, the time dependence of the ion pair monitored at 670 nm shows the rapid rise of absorbance within the response of the apparatus and further increase during ca. 10 ps, followed by the decrease with the time constant longer than a few tens of picoseconds. The rapid formation of the ion pair within the response of the apparatus is due to the excitation of the CT complex between BP and DMA formed in the ground state. On the other hand, the slower rise of the absorbance during ca. 10 ps may be attributed to the ion-pair production at the encounter of $^1BP^*$ and DMA, since the time constant of this rise of absorbance, (4.8±0.5) ps, is almost identical with the decay time of $^1BP^*$.

It should be noted here that the quenching rate constant of $^1BP^*$ by DMA is fairly large. The application of the simple analysis assuming the usual bimolecular reaction yields the rate constant of 1.1×10^{11} $M^{-1}s^{-1}$ which is 5 times larger than the diffusion-controlled rate constant, 2.0×10^{10} $M^{-1}s^{-1}$ in acetonitrile. Such a rapid reaction process in solution, which is called transient effect or nonstationary quenching, is effective in the case where the concentration of the quencher is high and the stationary bimolecular reaction rate is large. Taking the present experimental condition and the strength of the interaction between BP and DMA into account, this large rate constant for the quenching may be attributed to the rapid reaction of $^1BP^*$ with the neighboring DMA which has suitable oorientations for the electron transfer.

Time profile of the absorbance of $^3BP^*$ monitored at 525 nm is shown in Fig. 9(c), indicating that the rapid increase of the absorbance immediately after the excitation followed by slower rise and much slower decay of the absorbance. From Fig. 8, we can see clearly that the rapid rise at this wavelength may be attributed to the contribution from the absorbances of $^1BP^*$ and $^1(BP^-\cdots DMA^+)_{com}$ and slow rise during ca. 10 ps to the ISC of $^1BP^*$ to produce $^3BP^*$. The much slower decay of the absorbance may be due to the quenching process of $^3BP^*$ and the recombination of ion pairs. The rise time of $^3BP^*$, (4.5±0.5) ps, was identical with

the decay time of $^1BP^*$ within the experimental error and with the formation time of $^1(BP^-\cdots DMA^+)_{enc}$, which indicates that the formation of $^3BP^*$ by ISC and the electron transfer process is taking place competitively in $^1BP^*$.

Integrating above experimental results, we can summarize the electron transfer process of excited benzophenone in short time region as follows.

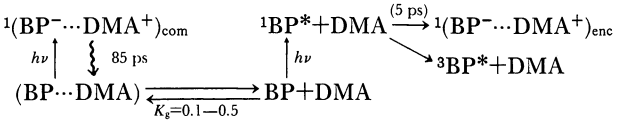

Scheme 3.

In this scheme, the ion pair produced by the excitation of the CT complex formed in the ground state, $^1(BP^-\cdots DMA^+)_{com}$, is discriminated from the ion pair produced at encounter of $^1BP^*$ with DMA, $^1(BP^-\cdots DMA^+)_{enc}$. More detailed discussions on the difference between two kinds of ion pair will be given later.

By the analysis of the spectrum immediately after the pulsed excitation into two components, $^1BP^*$ and $^1(BP^-\cdots DMA^+)_{com}$ and dividing each spectrum by the respective extinction coefficient, the fraction of the ion pair produced by the CT band excitation was obtained to be 0.30 and that of $^1BP^*$, 0.70. The yield of $^1(BP^-\cdots DMA^+)_{com}$ was fairly large, and it was concluded that about half of $^1BP^*$ resulted in the ion pair formation by encounter with DMA and remaining part of $^1BP^*$ was converted into $^3BP^*$, on the basis of the change of the lifetime of $^1BP^*$ and the concentration of each species obtained by the transient absorption spectrum. Consequently, only 35% of the absorbed energy was used to produce $^3BP^*$ in the acetonitrile solution containing 1.0 M DMA in the case of 355 nm excitation.

In order to elucidate dynamic behaviors and reaction yields of $^1(BP^-\cdots DMA^+)_{enc}$, transient absorption spectra of the acetonitrile solution containing 1.0 M DMA were measured by exciting the solution with picosecond 355 nm laser light (Fig. 10). A large amount of transient absorption due to ion pairs was clearly observed immediately after the excitation. This rapid ion pair formation is mainly due to the excitation of the CT complex and to the ET reaction between $^1BP^*$ and neighboring DMA. With the increase of the delay time after the excitation, the absorbance due to ion pairs decreases and reaches a plateau value which is due to the dissociated free ions as stated already in the previous sections.

In Fig. 11, we show the time profiles of $^3BP^*$, BPH radical, and ion pair absorbance, which were obtained by the analysis of the observed spectra into these components. It should be noted that the time profile of the ion pair absorbance comprises contributions from three kinds of ion pairs and dissociated ions. As indicated above, the initial yields of $^1(BP^-\cdots DMA^+)_{enc}$,

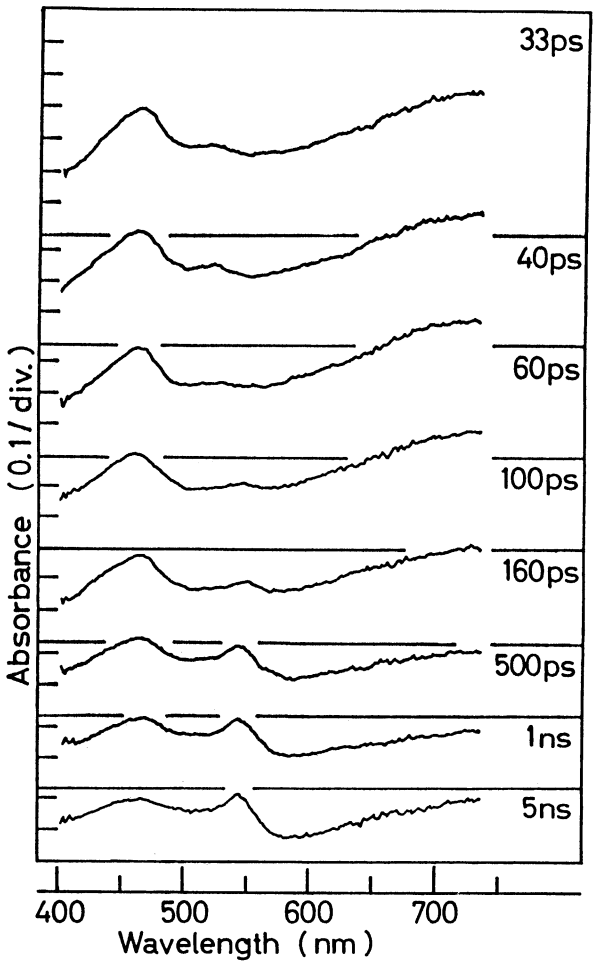

Fig. 10. Time-resolved transient absorption spectra of BP(0.01 M)-DMA(1.0 M) system in acetonitrile solution, excited with a picosecond 355 nm laser pulse.

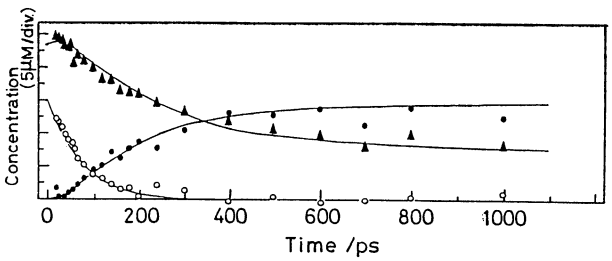

Fig. 11. Time profiles of $^3BP^*$ (○), BPH (●), and BP^- and DMA^+ (▲) of BP(0.01 M)-DMA(1.0 M) system in acetonitrile solution excited with a picosecond 355 nm laser pulse.

$^1(BP^-\cdots DMA^+)_{com}$, and $^3BP^*$ were determined by the femtosecond laser photolysis, respectively. In addition, the reaction pathways have been elucidated and their rate constants have been determined respectively for $^3BP^*$ and $^1(BP^-\cdots DMA^+)_{com}$. Taking these values into account, we analyzed time profiles by the curve-

Table 2. Properties of the Singlet Ion Pair, $^1(BP^- \cdots DMA^+)_{enc}$, in Acetonitrile Solutions with Various Concentrations of DMA. τ: Lifetime, ϕ_{PT} and k_{PT}: Reaction Yield and Rate Constant of the Proton Transfer, ϕ_{ID} and k_{ID}: Reaction Yield and Rate Constant of the Ionic Dissociation, ϕ_{CR} and k_{CR}: Reaction Yield and Rate Constant of the Charge Recombination

[DMA]	τ/ps	ϕ_{PT}	ϕ_{ID}	ϕ_{CR}	k_{PT}/s^{-1}	k_{ID}/s^{-1}	k_{CR}/s^{-1}
0.1 M	420	0.30	0.40	0.30	7.1×10^8	9.5×10^8	7.1×10^8
0.3 M	550	0.27	0.50	0.23	4.9×10^8	9.1×10^8	4.2×10^8
0.6 M	460	0.33	0.45	0.22	7.2×10^8	9.8×10^8	4.8×10^8
1.0 M	420	0.30	0.40	0.30	7.1×10^8	9.5×10^8	7.1×10^8
Average	(460±60)	0.30±0.024	0.44±0.048	0.26±0.043	$(6.6\pm1.1)\times10^8$	$(9.5\pm0.03)\times10^8$	$(5.8\pm1.5)\times10^8$

Table 3. Dependence of the Reaction Rate Constants of the Ion Pairs upon the Mode of Its Production

	k_{PT}/s^{-1}	k_{ID}/s^{-1}	k_{CR}/s^{-1}
$^3(BP^- \cdots DMA^+)_{enc}$	5.4×10^9	1.4×10^9	—
$^1(BP^- \cdots DMA^+)_{enc}$	6.6×10^8	9.5×10^8	5.8×10^8
$^1(BP^- \cdots DMA^+)_{com}$	$\ll10^8$	$\leq4\times10^8$	1.1×10^{10}

fitting method, where the lifetime and the reaction yields of $^1(BP^- \cdots DMA^+)_{enc}$ were varied as parameters. The solid lines in Fig. 11 were calculated by assuming that the lifetime, the reaction yield of the proton transfer, and the ionic dissociation yield of $^1(BP^- \cdots DMA^+)_{enc}$ were 420 ps, 0.3, and 0.4, respectively. The solid curve for ion pairs in this figure includes contributions from $^1(BP^- \cdots DMA^+)_{com}$, $^1(BP^- \cdots DMA^+)_{enc}$, and $^3(BP^- \cdots DMA^+)_{enc}$, and the calculated time profile for BPH radical also includes contributions from two formation pathways via $^1(BP^- \cdots DMA^+)_{enc}$ and $^3(BP^- \cdots DMA^+)_{enc}$.

As indicated in Fig. 11, the experimental values were reproduced by the calculated time dependences, and further, parameters for $^1(BP^- \cdots DMA^+)_{enc}$ were almost independent of the concentration of DMA as shown in Table 2. The averaged lifetime, and the reaction yields for the proton transfer, the ionic dissociation, and the charge recombination for $^1(BP^- \cdots DMA^+)_{enc}$ were 460 ps, 0.30, 0.44, and 0.26, respectively.

In Table 3, we list the rate constants for the proton transfer, k_{PT}, the ionic dissociation, k_{ID}, and the charge recombination, k_{CR}, for these three kinds of ion pairs. The rate constant for the charge recombination of $^3(BP^- \cdots DMA^+)_{enc}$ is not listed in this table, since this process has very small contribution, and hence, it was rather difficult to quantitatively determine the rate constant. The reaction rate constant for each process in Table 3 is quite different from each other depending on the mode of the production of the ion pair. This result indicates that the structure of the ion pair is different from each other and it does not change during its lifetime. In the following, we discuss the difference in detail.

4. The Difference of the Reactivity between the Singlet Ion Pairs Depending on the Mode of Their Production. As it is demonstrated above, the dynamic behaviors of the ion pair produced by the excitation of the CT complex formed in the ground state, $^1(BP^- \cdots DMA^+)_{com}$, was quite different from that produced by the electron transfer between $^1BP^*$ and DMA at encounter $^1(BP^- \cdots DMA^+)_{enc}$. This result is closely connected with the recent investigations which demonstrate the large difference in the dynamic behaviors of ion pairs (IP) of various donor acceptor systems depending on the mode of their production.[2,17,26] In those studies, charge recombination (CR) rate of IP produced by the excitation of the CT complex and its dependence on the energy gap between the IP state and the ground state, ΔG°_{ip}, have been examined in the case of various CT complexes covering a wide range of the energy gap by using femtosecond and picosecond laser photolysis. By these investigations, it has been revealed that the CR rate of IP produced by the CT complex excitation shows an essentially different energy gap dependence from the bell shape one obtained in the case of IP formed by charge separation at encounter in the fluorescence quenching reaction.[2-4,26] Further, the CR rate of IP produced by the CT complex excitation has been confirmed, in general, to be greater than that of IP formed by charge separation at encounter for the same donor (D) and acceptor (A) pair in acetonitrile.

From these findings, it has been suggested that the structure of IP's including the surrounding solvent is different from each other; the compact or contact ion pair (CIP) probably with no intervening solvent molecule between A^- and D^+ would be produced in the case of the excitation of the CT complex, while more loose IP (LIP) with intervening solvent molecules between A^- and D^+ (solvent-separated IP, SSIP) may be formed in the CS at encounter in the fluorescence quenching reaction. Moreover, from the results of those investigaitons, it has been concluded that the structures of these IP's could be maintained at least during several hundreds of picoseconds.

As described above, quite similar result has been obtained also in the present study on BP-DMA system. The CR rates of each ion pair have been obtained to be 1.1×10^{10} s^{-1} for $^1(BP^- \cdots DMA^+)_{com}$, and 5.8×10^8 s^{-1} for $^1(BP^- \cdots DMA^+)_{enc}$, respectively. The

tendency in the dependence of the CR rate on the mode of the production was similar to those various DA pairs. Moreover, the energy gap dependence of CR rate of the ion pair produced by the CT complex excitation,[17] predicts that the CR rate of the ion pair formed by the CT complex excitation, whose energy gap is similar to that of ($BP^-\cdots DMA^+$) ion pair, −2.5 eV, is in the order of 10^{10} s^{-1}. The CR rate of $^1(BP^-\cdots DMA^+)_{com}$, 1.1×0^{10} s^{-1}, is in a good agreement with it. Therefore, from the viewpoint of the ΔG°_{ip} dependence of the recombination rate, the behavior of the present $^1(BP^-\cdots DMA^+)_{com}$ is considered to be typical of the IP produced by the excitation of the CT complex. Hence, along with the interpretations presented for the IP's produced by excitation of various CT complexes, it is suggested that the present ion pair, $^1(BP^-\cdots DMA^+)_{com}$, has a rather rigid structure which cannot reorient to take a suitable structure for the proton transfer before the recombination, while $^1(BP^-\cdots DMA^+)_{enc}$ produced by the electron transfer between $^1BP^*$ and DMA at encounter has rather loose structure and, as a consequence of the difference in the structure and interaction between D^+ and A^- in the IP, is long-lived to form the suitable geometry for ketyl radical production.

Concerning the structure of the ion pair and its relation to the proton transfer between BP^- and DMA^+ in the IP, Peters and coworkers concluded that the electron-transfer reaction leading to the formation of the SSIP was followed by the change of the structure to the CIP where BPH formation by proton transfer took place.[12] This conclusion was based on the experimental results that the absorption maximum of BP^- was blue-shifted with increase of the delay time after the excitation. In their interpretation, the absorption band of BP^- with a maximum at 720 nm was assigned to the SSIP and that at 690 nm to the CIP. It should be noted that they derived above conclusion by assuming that the electron-transfer reaction took place exclusively at the encounter of $^3BP^*$ with DMA in concentrated solution (1—5 M), where, however, various kinds of ion pairs were produced according to our investigations.

In order to elucidate the mechanism responsible for this spectral shift, we have examined the transient absorption spectra of BP(0.01 M)-DMA(1.0 M) system in acetonitrile solution by picosecond 355 nm laser photolysis as shown in Fig. 12. We have observed time dependent shift of the spectral peak, which has reproduced the previous measurements.[12] However, the spectrum observed immediately after the excitation involves the contributions from the ion pair produced by the excitation of the CT complex, $^1(BP^-\cdots DMA^+)_{com}$, and from that formed by the electron transfer reaction between $^1BP^*$ and DMA, $^1(BP^-\cdots DMA^+)_{enc}$. Moreover, the BP^- band in the spectrum observed at a few ns after the excitation is due to the dissociated free ion. Therefore, in order to elucidate

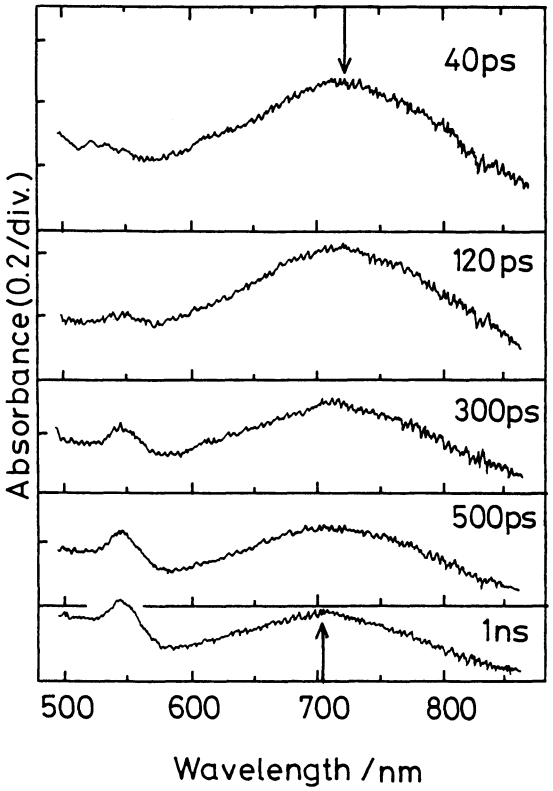

Fig. 12. Time-resolved transient absorption spectra of BP(0.01 M)-DMA(1.0 M) system in acetonitrile solution in longer wavelength region, excited with a picosecond 355 nm laser pulse.

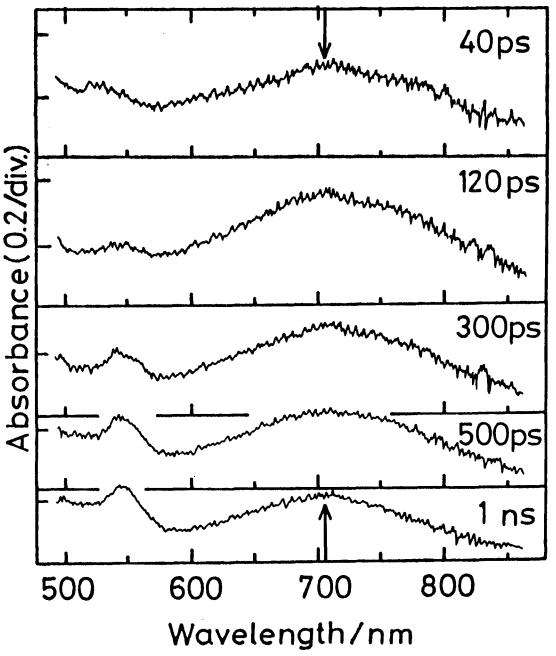

Fig. 13. Time-resolved transient absorption spectra of BP(0.01 M)-DMA(1.0 M) system in acetonitrile solution in longer wavelength region, excited with a picosecond 355 nm laser pulse. Contribution of $^1(BP^-\cdots DMA^+)_{com}$ is removed (see text).

the mechanism of the spectral shift, the contribution of the absorption band of $^1(BP^-\cdots DMA^+)_{com}$ should be removed, since $^1(BP^-\cdots DMA^+)_{com}$ shows an absorption maximum at 740 nm and during the decay process, no spectral shift can be observed (see Fig. 6). Figure 13 shows the transient absorption spectra of the same solution, where, however, the spectrum due to $^1(BP^-\cdots DMA^+)_{com}$ was subtracted from Fig. 12 in such a manner that the initial yield of $^1(BP^-\cdots DMA^+)_{com}$ and the decay time constant (85 ps) were set to those indicated in Scheme 3. In Fig. 13, such a clear spectral shift as in Fig. 12 can not be observed, though the rather broad absorption spectrum of BP^- observed immediately after the excitation gradually changes its spectral shape to a sharper one. Accordingly, it may be concluded that the observed spectral shift is mainly due to the decay of the absorption band of $^1(BP^-\cdots DMA^+)_{com}$ as well as the production of the dissociated ions. It should be emphasized here that the absorption band of BP^- with peak at 690 nm should not be ascribed to the contact ion pair, since the blue-shifted absorption observed at a few ns after excitation is due to the dissociated BP^-.

Integrating above results and discussions, it may be concluded that the ion pair which is produced by the CT band excitation and whose structure is suggested to be a contact form shows an absorption maximum at longer wavelength region (740 nm), while the dissociated BP^-, $^1(BP^-\cdots DMA^+)_{enc}$ and $^3(BP^-\cdots DMA^+)$ show maximum around 690—710 nm. The fact that the absorption maximum of $^1(BP^-\cdots DMA^+)_{enc}$ and that of $^3(BP^-\cdots DMA^+)_{enc}$ is close to that of the free BP^- ion but is different from that of $^1(BP^-\cdots DMA^+)_{com}$ strongly suggests that the solvation structure of the ion pair produced at encounter is closer to that of free BP^- than that of $^1(BP^-\cdots DMA^+)_{com}$.

5. The Difference of the Reactivity between $^3(BP^-\cdots DMA^+)_{enc}$ and $^1(BP^-\cdots DMA^+)_{enc}$. As stated in previous sections, the reaction mechanism of the ketyl radical formation in the case of BP-DMA system has been confirmed to be the successive process of IP formation followed by proton transfer not only in the case of the hydrogen abstraction of $^3BP^*$ but also $^1BP^*$. However, their reaction rate constants are quite different from each other. The large difference of the charge recombination rate constant, k_{CR}, between two kinds of ion pairs can be ascribed to the difference of the spin multiplicity of the ion pair. On the other hand, the rate constant of the proton transfer, k_{PT}, of $^3(BP^-\cdots DMA^+)_{enc}$ was almost 8 times as large as that of $^1(BP^-\cdots DMA^+)_{enc}$, which cannot be ascribed solely to the difference of the spin multiplicity. This difference of k_{PT} between the two kinds of IP's may be related also to the difference of the structure of the ion pair such as the mutual distance and the orientation of ions in the pair including the surrounding solvents. Although it is rather difficult at the present stage of the investigation to give any definite conclusion on the structures of these ion pairs, it is plausible that the ion pair produced through the electron transfer reaction between $^1BP^*$ and DMA has a more specific structure since the electron transfer process between them is mainly due to the nonstationary quenching and, as a consequence, the mutual distance and the orientation of ions in the pair may be somewhat different from those of the ion pairs produced via the stationary diffusion process. In addition, the difference of electronic structure of $^1BP^*$ from $^3BP^*$ may affect to some extent the mutual configurations between donor and acceptor at the encounter.

Especially, the rate constant for the ionic dissociation process seems to reflect directly the structure of the ion pair and the attractive interaction between two oppositely charged species, since this process is regarded as the thermal diffusive motion of ions in the Coulombic field in the classical sense where the ions are treated as small charged spheres in the dielectic fluids. According to this classical description, decrease of the rate constant may be interpreted as the decrease in the distance between two charged particles. It should be noted that this description is a very approximate one and more detailed structures such as mutual orientations of actual molecular ions including the surrounding solvents should be included in the interpretations of the difference in k_{ID}. In spite of these limitations, the variation of k_{ID} depending on the mode of the ion pair formation directly suggests the difference of the structure of the ion pair and indicates that the ion pair which has small dissociation rate constant may have rather tight structure.

In addition to this, the geometric requirement for the proton or the hydrogen atom transfer processes seems to be more severe compared to that for the electron transfer reaction, since the conformatinal requirement for the latter process is dependent on the electronic molecular orbital spreading over a rather wide region, while the sites for the transfer of proton or hydrogen in the donor and the acceptor are limited within the narrow region. Hence, the difference in the structure of the ion pair seems to strongly affect the proton transfer probability.

It is worth noting that k_{PT} increases with increase of k_{ID} in the three kinds of ion pairs as listed in Table 3. As discussed above, the ion pair which has large k_{ID} seems to have a rather loose structure and, accordingly, may be able to undergo a small change of mutual orientations of ions in the pair, which will facilitate the proton transfer to some extent.

6. The Different Reaction Mechanism Depending on the Nature of the Amine. As discussed above, the mechanism of the hydrogen abstraction of $^3BP^*$ from DMA in acetonitrile solution is the successive reaction as given by the Scheme 2, while the hydrogen abstraction process of $^3BP^*$ from DPA was the direct abstraction competing with the production of the stable ion pair.[16] However, we have confirmed that the reac-

tion mechanism of the hydrogen abstraction of ^{3}BP* from DMA in 2-propanol is not the successive one but can be described by the direct abstraction mechanism. Moreover, we have made also more systematic studies concerning effects of various factors upon the photochemical primary process of benzophenone-amine systems in various solvents of different polarities. That is, we have examined the effect of the oxidation potential of amine, the effect of the difference in primary, secondary and tertiary amine, and the effect of changing the reduction potential of benzophenone by substitution in phenyl rings on the reaction mechanisms. Results of these investigations indicate the crucial importance of the transient charge transfer interaction in a short-lived intermediate formed in the excited benzophenone-amine systems as the factor determining the reaction mechanism. Nevertheless, the transient charge transfer or electron transfer interaction in the excited benzophenone-amine systems can lead to quite different result in the hydrogen abstraction reaction depending upon the mutual distance and configurations of reactants pair in the intermediate state as we have discussed in some detail in the above sections in the case of benzophenone-DMA system and also upon the nature of amine including its oxidation potential and difference in primary, secondary, tertiary amine as well as the nature of solvent.[32] It is rather difficult at present to derive a clear conclusion on the underlying mechanism leading to such difference in the hydrogen abstraction reaction depending on the nature of amine and the solvent. Roughly speaking, it is suggested that the structure including both reactants at the encounter collision which is controlled also to some extent by the nature of the solvent and the oxidation potential of the amine affects the reaction mechanism.

Concerning the structure and dynamics of the molecular complex produced through the photoinduced charge transfer or electron transfer reaction, it was reported that the electronic state of the typical singlet exciplex system such as pyrene-DMA was strongly dependent on the polarity of the solvent and this dependence on the solvent polarity was not accounted for by the mere stabilization of the single electronic state by the solvation but by the gradual change of the electronic structure of the complex depending on the solvent polarity.[33] In addition, it was revealed that the fluorescent exciplex and nonfluorescent solvated ion pairs was produced competitively, depending upon the solvent polarity, from the nonrelaxed CT state immediately after the electron transfer between excited singlet state of pyrene and DMA.[34] Integrating those previous results and the present ones, it is suggested that the mutual geometry such as orientation and distance including the surrounding solvent at the encounter between the reactants strongly affect the subsequent behaviors of the transient charge transfer or the ion pair state. On this problem, we are now investigating the system where mutual configurations are restricted and results of which will be published in the forthcoming paper.

N. M. acknowledges the support by a Grant-in-Aid (No. 62065006) from the Ministry of Education, Science and Culture.

References

1) N. Mataga, *Pure. Appl. Chem.*, **56**, 1255 (1984).
2) N. Mataga, *Acta Pyhs. Pol.*, **71**, 767 (1987).
3) N. Mataga, "Photochemical Energy Conversion," Elsevier, Amsterdam (1988), p. 32.
4) N. Mataga, H. Miyasaka, T. Asahi, S. Ojima, and T. Okada, "Ultrafast Phenomena VI," Springer-Verlag, Berlin (1988), p. 511.
5) A. Backett and G. Porter, *Trans. Faraday Soc.*, **59**, 2038 (1963).
6) G. Porter and M. R. Topp, *Proc. R. Soc. London, Ser. A*, **315**, 163 (1970).
7) S. G. Cohen, A. Parola, and G. H. Rarsons, *Chem. Rev.*, **73**, 1411 (1973), and references cited therein.
8) S. Arimitsu and H. Masuhara, *Chem. Phi Lett.*, **22**, 543 (1973).
9) S. Arimitsu, H. Masuhara, N. Mataga, and H. Tsubomura, *J. Phys. Chem.*, **79**, 1255 (1975).
10) K. S. Peters, S. C. Felich, and C. G. Shaefer, *J. Am. Chem. Soc.*, **102**, 5701 (1980).
11) C. G. Shaefer and K. S. Peters, *J. Am. Chem. Soc.*, **102**, 7567 (1980).
12) J. D. Simon and K. S. Peters, *J. Am. Chem. Soc.*, **103**, 6403 (1981).
13) L. E. Manring and K. S. Peters, *J. Am. Chem. Soc.*, **107**, 6452 (1985).
14) M. Hoshino and H. Shizuka, *J. Phys. Chem.*, **91**, 714 (1987).
15) H. Hoshino and M. Kogure, *J. Phys. Chem.*, **93**, 728 (1989).
16) H. Miyasaka and N. Mataga, *Bull. Chem. Soc. Jpn.*, **63**, 131 (1990).
17) a) N. Mataga, Y. Kanda, T. Asahi, H. Miyasaka, T. Okada, and T. Kakitani, *Chem. Phys.*, **127**, 239 (1988); b) T. Asahi and N. Mataga, *J. Phys. Chem.*, **93**, 6575 (1989); c) T. Asahi and N. Mataga, *ibid.*, in press.
18) H. Masuhara, N. Ikeda, H. Miyasaka, and N. Mataga, *J. Spectros. Soc. Jpn.*, **31**, 19 (1982).
19) H. Miyasaka, H. Masuhara, and N. Mataga, *Laser Chem.*, **1**, 357 (1985).
20) Y. Hirata, N. Mataga, Y. Sakata, and S. Misumi, *J. Phys. Chem.*, **86**, 1508 (1982).
21) H. Miyasaka, S. Ojima, and N. Mataga, *J. Phys. Chem.*, **93**, 3380 (1989).
22) R. V. Bensasson and J.-C. Gramain, *J. Chem. Soc., Faraday Trans. 2*, **76**, 1801 (1980).
23) H. Hiratsuka, T. Yamazaki, Y. Maekawa, T. Hidaka, and Y. Mori, *J. Phys. Chem.*, **90**, 774 (1986).
24) T. Shida, Y. Nosaka, and T. Kato, *J. Phys. Chem.*, **82**, 695 (1978).
25) T. Shida, S. Iwata, and M. Imamura, *J. Phys. Chem.*, **78**, 741 (1974).
26) N. Mataga, T. Asahi, Y. Kanda, T. Okada, and T. Kakitani, *Chem. Phys.*, **127**, 249 (1988).

27) H. Miyasaka, K. Kamada, K. Morita, and N. Mataga, to be published.
28) J. D. Simon and K. S. Peters, *J. Am. Chem. Soc.*, **105**, 4875 (1983).
29) R. K. Huddleston and J. R. Miller, *Radiat. Phys. Chem.*, **17**, 383 (1981).
30) C. Pac, K. Mizuno, T. Tosa, and H. Sakurai, *J. Chem. Soc., Perkin Trans. 1*, 561 (1974).
31) R. M. Hochstrasser, H. Lutz, and G. W. Scott, *Chem. Phys. Lett.*, **24**, 162 (1974).
32) T. Miyasaka, K. Kamada, K. Morita, M. Kiri, and N. Mataga, to be published.
33) N. Mataga, T. Okada, and N. Yamamoto, *Chem. Phys. Lett.*, **1**, 119 (1967).
34) Y. Hirata, Y. Kanda, and N. Mataga, *J. Phys. Chem.*, **87**, 1659 (1983).